

# The Trace Criterion for Kernel Bandwidth Selection for Support Vector Data Description

Arin Chaudhuri<sup>a,\*</sup>, Carol Sadek<sup>a</sup>, Deovrat Kakde<sup>a</sup>, Wenhao Hu<sup>b,1</sup>, Hansi Jiang<sup>a</sup>, Seunghyun Kong<sup>a</sup>, Yuwei Liao<sup>a</sup>, Sergiy Peredriy<sup>a</sup>, Haoyu Wang<sup>a</sup>

<sup>a</sup>*Internet of Things, SAS Institute Inc., Cary, NC, 27513*

<sup>b</sup>*2250 Latham St Apt 51, Mountain View, CA 94040*

---

## Abstract

Support vector data description (SVDD) is a popular anomaly detection technique. The SVDD classifier partitions the whole data space into an *inlier* region, which consists of the region *near* the training data, and an *outlier* region, which consists of points *away* from the training data. The computation of the SVDD classifier requires a kernel function, for which the Gaussian kernel is a common choice. The Gaussian kernel has a bandwidth parameter, and it is important to set the value of this parameter correctly for good results. A small bandwidth leads to overfitting such that the resulting SVDD classifier overestimates the number of anomalies, whereas a large bandwidth leads to underfitting and an inability to detect many anomalies. In this paper, we present a new unsupervised method for selecting the Gaussian kernel bandwidth. Our method exploits a low-rank representation of the kernel matrix to suggest a kernel bandwidth value. Our new technique is competitive with the current state of the art for low-dimensional data and performs extremely well for many classes of high-dimensional data. Because the mathematical formulation of SVDD is identical with the mathematical formulation of one-class support vector machines (OCSVM) when the Gaussian kernel is used, our method is equally applicable to Gaussian kernel bandwidth tuning for OCSVM.

*Keywords:* Support Vector Data Description, SVDD, One Class Support Vector Machines, OCSVM, Gaussian Kernel, Automatic Tuning

---

\*Corresponding author

*Email address:* [arin.chaudhuri@sas.com](mailto:arin.chaudhuri@sas.com) (Arin Chaudhuri)

<sup>1</sup>This work was done when the author was with SAS Institute Inc.

---

## 1. Introduction

In this section we provide a brief description of the support vector data description technique. Our description follows the description given in [16] and [7, 3].

Support vector data description (SVDD) is a machine learning technique that is used for single-class classification and anomaly detection. First introduced by Tax and Duin [16], SVDD’s mathematical formulation is almost identical to the one-class variant of support vector machines: one-class support vector machines (OCSVM), which is attributed to Schölkopf et al. [14]. The use of SVDD is popular in domains in which the majority of data belong to a single class and no distributional assumptions can be made. For example, SVDD is useful for analyzing sensor readings from reliable equipment for which almost all the readings describe the equipment’s normal state of operation.

SVDD provides a geometric description of the observed data. The SVDD classifier assigns a *distance* to each point in the domain space; the distance measures the separation of that point from the training data. During scoring, any observation found to be at a *large* distance from the training data might be an anomaly, and the user might choose to generate an alert.

Several researchers have proposed using SVDD for multivariate process control [15, 2]. Other applications of SVDD involve monitoring condition of machines [18, 21] and image classification [12, 8].

### 1.1. Mathematical Formulation

In this section, we describe the mathematical formulation of SVDD following [16, 3].

#### 1.1.1. Normal Data Description

The SVDD model for normal data description builds a sphere that contains most of the data within a small radius. Given observations  $x_1, \dots, x_n \in \mathbb{R}^p$ , we need to solve an optimization problem to determine the sphere. We present the optimization problem in its primal and dual forms below.

## Primal Form

### Objective

$$\min R^2 + C \sum_{i=1}^n \xi_i, \quad (1)$$

### Subject to

$$\|x_i - a\|^2 \leq R^2 + \xi_i, \forall i = 1, \dots, n, \quad (2)$$

$$\xi_i \geq 0, \forall i = 1, \dots, n, \quad (3)$$

### Where

- $x_i \in \mathbb{R}^p, i = 1, \dots, n$  represent the training data,
- $R$  is the radius and represents the decision variable,
- $\xi_i$  is the slack for each variable,
- $a$  is the center (a decision variable),
- $C$  is the penalty constant that controls the trade-off between the radius and the errors.

## Dual Form

The dual formulation is obtained using Lagrange multipliers.

### Objective

$$\max \sum_{i=1}^n \alpha_i \langle x_i, x_i \rangle - \sum_{i,j} \alpha_i \alpha_j \langle x_i, x_j \rangle, \quad (4)$$

### Subject to

$$\sum_{i=1}^n \alpha_i = 1,$$
$$0 \leq \alpha_i \leq C, \forall i = 1, \dots, n$$

### Where

$\alpha_i \in \mathbb{R}$  are the Lagrange constants and  $C$  is the penalty constant.

## Duality Information

The optimal dual parameters  $\alpha_i$  are extremely useful as they can be used to determine the minimal radius sphere which surrounds the data and the position of the points in the data relative to this sphere.

Let  $SV_{< C}$  denote the set  $\{x_j : 0 < \alpha_j < C\}$  and choose any  $x_k \in SV_{< C}$ . The radius of the sphere  $\mathbf{R}$  is given by

$$\mathbf{R}^2 = \langle x_k, x_k \rangle - 2 \sum_i \alpha_i \langle x_i, x_k \rangle + \sum_{i,j} \alpha_i \alpha_j \langle x_i, x_j \rangle. \quad (5)$$

The value of  $\mathbf{R}^2$  does not depend on the choice of  $x_k \in SV_{< C}$ .

The center of the sphere  $\mathbf{a}$  is given by

$$\mathbf{a} = \sum_{i=1}^n \alpha_i x_i \quad (6)$$

The points  $x_i$  for which the corresponding  $\alpha_i$  equal 0 lie inside this sphere, that is,

$$\|x_i - \mathbf{a}\| < \mathbf{R} \iff \alpha_i = 0. \quad (7)$$

The points  $x_i$  for which the corresponding  $\alpha_i$  lie between 0 and  $C$  are on the boundary of this sphere.

$$\|x_i - \mathbf{a}\| = \mathbf{R} \iff 0 < \alpha_i < C$$

The remaining points lie outside the sphere.

$$\|x_i - \mathbf{a}\| > \mathbf{R} \iff \alpha_i = C \quad (8)$$

Any  $x_i$  for which the corresponding  $\alpha_i > 0$  is called a support vector.

## Scoring

For any point  $z$ , its distance from the center of the sphere  $\text{dist}^2(z) = \|z - \mathbf{a}\|^2$  equals

$$\begin{aligned} \text{dist}^2(z) &= \left\| z - \sum_i \alpha_i x_i \right\|^2 \\ &= \langle z, z \rangle - 2 \sum_i \alpha_i \langle x_i, z \rangle + \sum_{i,j} \alpha_i \alpha_j \langle x_i, x_j \rangle. \end{aligned} \quad (9)$$

If  $\text{dist}^2(z) > R^2$  then  $z$  is designated as an outlier.

### Problems with the Normal Data Description

The spherical data boundary can include a significant amount of space that has a sparse distribution of training observations. Using this model to score can lead to a lot of false positives. Hence, instead of a spherical shape, a compact bounded outline around the data is often desired. Such an outline should approximate the shape of the single-class training data. This is possible by using kernel functions. The SVDD formulation with kernel functions leads to the flexible data description which is described next.

#### 1.1.2. Flexible Data Description

The support vector data description is made flexible by replacing the inner product  $\langle x_i, x_j \rangle$  with a suitable kernel function  $K(x_i, x_j)$ . The Gaussian kernel function used in this paper is defined as

$$K_s(x, y) = \exp\left(-\frac{\|x - y\|^2}{2s^2}\right); \quad (10)$$

where  $s$  is the Gaussian bandwidth parameter.

The modified mathematical formulation of SVDD with a kernel function  $K$  is

<p><b>Objective</b></p> $\max \sum_{i=1}^n \alpha_i K(x_i, x_i) - \sum_{i,j} \alpha_i \alpha_j K(x_i, x_j), \quad (11)$ <p><b>Subject to</b></p> $\sum_{i=1}^n \alpha_i = 1,$ $0 \leq \alpha_i \leq C, \forall i = 1, \dots, n$ <p><b>Where</b>  <math>\alpha_i \in \mathbb{R}</math> are the Lagrange constants, and <math>C</math> is the penalty constant.</p>
---

In perfect analogy with the previous section, any  $x_i$  for which  $\alpha_i = 0$  is an *inside* point and any  $x_i$  for which  $\alpha_i > 0$  is called a support vector.

$SV_{< C}$  is similarly defined as  $\{x_j : 0 < \alpha_j < C\}$  and given any  $x_k \in SV_{< C}$

the threshold  $R^2$  is calculated as

$$R^2 = K(x_k, x_k) - 2 \sum_i \alpha_i K(x_i, x_k) + \sum_{i,j} \alpha_i \alpha_j K(x_i, x_j) \quad (12)$$

The value of  $R^2$  does not depend on which  $x_k \in SV_{< C}$  is used.

### Scoring

For any observation  $z$ , the distance  $\text{dist}^2(z)$  is calculated as follows:

$$\text{dist}^2(z) = K(z, z) - 2 \sum_i \alpha_i K(x_i, z) + \sum_{i,j} \alpha_i \alpha_j K(x_i, x_j) \quad (13)$$

Any point  $z$  for which  $\text{dist}^2(z) > R^2$  is designated as an outlier.

#### 1.2. Overview

In practice, SVDD is almost always computed by using the Gaussian kernel function, and it is important to set the value of bandwidth parameter correctly. A small bandwidth leads to overfitting, and the resulting SVDD classifier overestimates the number of anomalies. A large bandwidth leads to underfitting, and the classifier fails to detect many anomalies.

In this paper, we introduce the trace criterion method for Gaussian bandwidth selection. The computation of the trace criterion consists of finding the inflection point of a smooth function of the bandwidth parameter. The computation terminates quickly when standard nonlinear optimization methods such as Newton-Raphson are used. This method is efficient for moderately large data sets: we have successfully applied the trace criterion method to datasets with two million observations. The trace criterion has also been available in commercial software since May 2019 [13].

Our results show that the trace criterion is competitive with the current state of the art, it can be computed quickly and simulation studies show that this method is very accurate for high-dimensional data.

These properties make the trace criterion method a good bandwidth selection technique. However, unsupervised bandwidth tuning is an extremely difficult problem, so it is quite possible that there is a class of data sets for which the trace criterion method does not give good results.

The rest of the paper is organized as follows. Section 2 defines the trace criterion method for bandwidth tuning; in section 3, we introduce alternative bandwidth selection methods; and in section 4 we compare the different bandwidth selection methods on a variety of simulated and real data.

## 2. The Trace Criterion for Bandwidth Selection

### 2.1. Parameter Tuning Using Inflection Points

Parameter tuning for unsupervised learning methods such as clustering and one-class classification can be difficult when external validation data are not available, as is quite frequently the case. A popular method for parameter tuning in such cases is to look at the values of a “validation measure” as a function of the hyperparameter of interest, and choose the value of the hyperparameter where the function has an inflection point [1]. For a specific example, consider the problem of determining the number of clusters for  $K$ -means.  $SSQ$  (the sum of the squared distance of each point in the training data from the cluster center closest to it) can be taken as a validation measure. If the number of clusters is held fixed, then a lower value of  $SSQ$  indicates better clustering. Let  $SSQ(K)$  denote the value of  $SSQ$  for the clustering that is suggested by  $K$ -means with  $K$  clusters. As  $K$  increases,  $SSQ(K)$  decreases, so you cannot choose the number of clusters as  $K = \operatorname{argmin}_K SSQ(K)$  because doing so would suggest as many clusters as the number of points in the training data. However, it is observed that the value of  $K$  at which the function  $K \rightarrow SSQ(K)$  has an inflection point is quite frequently a good choice for the number of clusters. The inflection point of other validation measures such as the silhouette coefficient is also used to determine the number of clusters [1].

We will now propose a validation measure for SVDD whose inflection point provides our suggested bandwidth.

### 2.2. Validation Measure for Trace Criterion

Assume we have a training data set  $x_1, \dots, x_N$  that consists of  $N$  distinct points in  $\mathbb{R}^p$  and we propose the trace criterion as a kernel bandwidth value for training this data set. The trace criterion uses the Nyström approximation of a kernel matrix, so we start by describing the Nyström approximation.

#### 2.2.1. Nyström Approximation of the Kernel Matrix

In kernel methods, including SVDD, the objective function to be optimized depends on the training data through the kernel matrix  $K = (K(x_i, x_j))$ . Because this matrix has  $N^2$  elements, where  $N$  is the number of observations, it is impossible to work with the entire kernel matrix even for moderate values of  $N$ . The Gaussian kernel matrix is always positive semidefinite, and it typically has a rapidly decaying spectrum. The rapidly decaying spectrum

can be exploited to create a low-rank positive semidefinite approximation  $\tilde{K}$  of  $K$  by replacing all the eigenvalues in the spectral decomposition of  $K$  below a certain threshold with 0 [19].  $\tilde{K}$  has a square root of low rank, that is,  $\tilde{K} = GG^T$ , where  $G$  is an  $N \times r$  matrix with  $r \ll N$ . Since  $K \approx \tilde{K}$ ,  $G$  is considered to be an approximate low-rank square root of  $K$ . In many cases, computation of expressions that involve  $K$  can be made tractable by replacing  $K$  with  $GG^T$ . However, it is not feasible to compute  $G$  such that  $K \approx GG^T$  by using the eigendecomposition of  $K$  when  $N$  is large.

The Nyström methods form a class of popular methods to compute a low-rank representation of  $K$  even when  $N$  is large. We use a variant of the Nyström method as described in [22] to construct a validation measure whose inflection point will be suggested as the bandwidth.

Given data  $x_1, \dots, x_N$  in  $\mathbb{R}^p$  and an integer  $0 < r \ll N$ , let  $z_1, z_2, \dots, z_r$  be distinct *landmark points* in  $\mathbb{R}^p$ . The landmark points are chosen so that they are evenly distributed within the training data. Following [22], we choose  $z_1, \dots, z_r$  as the cluster centers that are obtained from a  $K$ -means clustering with  $r$  clusters of the training data.

From the theory of reproducing kernel Hilbert spaces (RKHS), we know that for any  $s > 0$  there is a Hilbert space  $\mathcal{H}_s$  and a mapping  $\Phi: \mathbb{R}^p \rightarrow \mathcal{H}_s$  such that for any  $x, y \in \mathbb{R}^p$  we have  $\langle \Phi(x), \Phi(y) \rangle_s = \exp -\frac{\|x - y\|^2}{2s^2} := K_s(x, y)$ , where  $\langle \cdot, \cdot \rangle_s$  denotes the inner product on  $\mathcal{H}_s$  and  $\|\cdot\|_s$  denotes the norm on  $\mathcal{H}_s$ .

Let  $V_0 \subseteq \mathcal{H}_s$  denote the subspace spanned by  $\Phi(z_1), \dots, \Phi(z_r)$ . Note that  $V_0$  is a finite-dimensional and hence closed subspace of  $\mathcal{H}_s$  of dimension exactly  $r$ . Given  $x \in \mathbb{R}^p$ , let  $\hat{\Phi}(x)$  denote the projection of  $\Phi(x)$  on  $V_0$ . In the Nyström methods, the kernel matrix  $(K_s(x_i, x_j))_{i,j=1}^N = (\langle \Phi(x_i), \Phi(x_j) \rangle_s)_{i,j=1}^N$  is approximated by  $(\langle \hat{\Phi}(x_i), \hat{\Phi}(x_j) \rangle_s)_{i,j=1}^N$ , a rank  $r$  matrix that has a low-dimensional square root that can be easily computed.

### 2.2.2. Trace Criterion validation measure

We use the projected values  $\hat{\Phi}(x)$  for a different purpose. We use the discrepancy between  $\hat{\Phi}(x)$  and  $\Phi(x)$  for  $x$  in the training data to come up with a validation measure.

From usual least square arguments, we know that for any  $x \in \mathbb{R}^p$ , we



have  $\widehat{\Phi}(x) = \sum_{i=1}^r \gamma_i \Phi(z_i)$ , where  $\gamma_1, \dots, \gamma_r$  are such that

$$\langle \Phi(x) - \sum_{i=1}^r \gamma_i \Phi(z_i), \Phi(z_k) \rangle = 0 \quad \text{for } k = 1, \dots, r.$$

This implies the normal equations,

$$K_s(x, z_k) = \sum_{i=1}^r \gamma_i K_s(z_i, z_k) \quad \text{for } k = 1, \dots, r,$$

and implies that  $\gamma_i$  can be explicitly computed as

$$\begin{pmatrix} \gamma_1 \\ \gamma_2 \\ \dots \\ \gamma_r \end{pmatrix} = \begin{pmatrix} 1 & K_s(z_1, z_2) & \dots & K_s(z_1, z_r) \\ K_s(z_1, z_2) & 1 & \dots & K_s(z_2, z_r) \\ \dots & \dots & \dots & \dots \\ K_s(z_r, z_1) & K_s(z_r, z_2) & \dots & 1 \end{pmatrix}^{-1} \begin{pmatrix} K_s(x, z_1) \\ K_s(x, z_2) \\ \dots \\ K_s(x, z_r) \end{pmatrix}. \quad (14)$$

Since  $\widehat{\Phi}(x)$  and  $\Phi(x) - \widehat{\Phi}(x)$  are orthogonal, the squared norm of the residual is given by

$$\begin{aligned} \rho(x, s) &:= \|\widehat{\Phi}(x) - \Phi(x)\|_s^2 \\ &= \|\Phi(x)\|_s^2 - \|\widehat{\Phi}(x)\|_s^2 \\ &= 1 - \left\| \sum_{i=1}^r \gamma_i \Phi(z_i) \right\|_s^2. \end{aligned}$$

This shows that  $0 \leq \rho(x, s) \leq 1$ . Let  $\psi(x, s) := 1 - \rho(x, s)$ . The closer  $\psi(x, s)$  is to 1, the lower the residual error is. From the preceding expression for  $\gamma_i$  we can see that

$$\psi(x, s) = \begin{pmatrix} K_s(x, z_1) \\ K_s(x, z_2) \\ \dots \\ K_s(x, z_r) \end{pmatrix}^T \begin{pmatrix} 1 & K_s(z_1, z_2) & \dots & K_s(z_1, z_r) \\ K_s(z_1, z_2) & 1 & \dots & K_s(z_2, z_r) \\ \dots & \dots & \dots & \dots \\ K_s(z_r, z_1) & K_s(z_r, z_2) & \dots & 1 \end{pmatrix}^{-1} \begin{pmatrix} K_s(x, z_1) \\ K_s(x, z_2) \\ \dots \\ K_s(x, z_r) \end{pmatrix}. \quad (15)$$

So, given training data  $x_1, \dots, x_N$ , if we define

$$g(s) := \frac{1}{N} \sum_{i=1}^N \psi(x_i, s),$$

then  $g(s)$  is a measure of the loss of accuracy due to projection into  $V_0$ , where  $g(s)$  lies between 0 and 1 for each  $s > 0$ . *Higher* values of  $g(s)$  indicate *lower* loss in precision due to projection into  $V_0$ . In particular, if  $g(s) = 1$ , there is absolutely no loss of precision. That is,

$$\widehat{\Phi}(x_i) = \Phi(x_i) \text{ for } 1 \leq i \leq N.$$

It is empirically observed that typically  $g(s)$  increases as  $s$  increases (that is,  $g'(s) > 0$ ). Moreover  $h(s) = g'(s)$  is unimodal: it initially increases until it reaches its maximum value, and then decreases. So  $g(s)$  typically has a well-defined inflection point where  $h(s)$  takes its maximum value. See Figure 1 for the graph of a typical plot of  $g()$  and  $h()$ .

The trace criterion method suggests using  $s^* = \operatorname{argmax}_{s>0} h(s)$  as the bandwidth that empirical observations suggest coincides with the inflection point of  $g$  in most cases.

Even though  $h(s)$  is a scalar function, it is defined in terms of matrix operations and we can come up with an explicit closed form for  $h(s)$  by using usual rules of matrix differential calculus [9].

Let  $U(s)$  denote the  $r \times r$  kernel matrix of representative points  $(K_s(z_i, z_j))_{i,j=1}^r$ . Its element-by-element derivative is given by the  $r \times r$  matrix,

$$U'(s) = \frac{1}{s^3} (\|z_i - z_j\|^2 K_s(z_i, z_j))_{i,j=1}^r.$$

For  $1 \leq i \leq N$ , let  $W_i(s) = (K_s(x_i, z_k))_{k=1}^r$  denote a  $r \times 1$  column vector. Then its element-by-element derivative is given by the  $r \times 1$  column vector,

$$W'_i(s) = \frac{1}{s^3} (\|x_i - z_k\|^2 K_s(x_i, z_k))_{k=1}^r.$$

Then we have

$$g(s) = \frac{\sum_{i=1}^N W_i^T(s) U^{-1}(s) W_i(s)}{N},$$

and hence

$$h(s) = g'(s) = \frac{2 \sum_{i=1}^N W_i^T(s) U^{-1}(s) W'_i(s)}{N} - \frac{\sum_{i=1}^N W_i^T(s) U^{-1}(s) U'(s) U^{-1}(s) W_i(s)}{N}.$$

Let  $B_i(s) := U^{-1}(s) W_i(s)$ . Then the preceding equation simplifies to

$$h(s) = \frac{2 \sum_{i=1}^N B_i^T(s) W_i(s)}{N} - \frac{\sum_{i=1}^N B_i^T(s) U'(s) B_i(s)}{N}. \quad (16)$$

From (16), it is apparent that  $h(s)$  is differentiable on  $0 < s < \infty$  so we can use standard nonlinear optimization methods such as Newton-Raphson to maximize it.

The cost of evaluating  $h(s)$  is  $\mathcal{O}(Nr^2)$ , which is tractable because  $r \ll N$ .

We have to choose the number of representative points,  $r$ , for applying the trace criterion method. We have observed that  $r = 5$  gives a good result for most data sets, and we have used the trace criterion with  $r = 5$  throughout this paper unless explicitly stated otherwise.

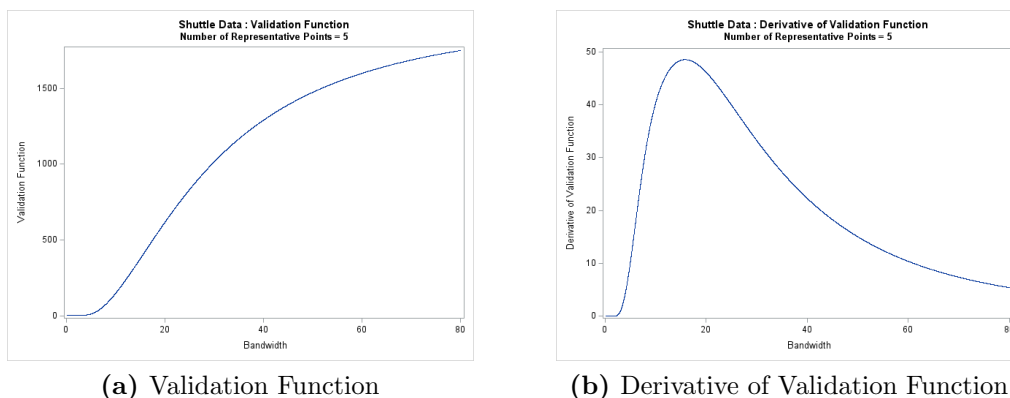


**Figure 1:** Plot of a validation function and its derivative

### 3. Alternative Methods

Because SVDD is an unsupervised learning technique it is not possible to use cross-validation to determine a suitable bandwidth value in general. So it is desirable to use automatic, unsupervised bandwidth selection techniques.

Such bandwidth selection methods for SVDD fall into two groups:

1. Intrinsic methods: These methods suggest a bandwidth value solely on the basis of training data. Some intrinsic methods provide a closed-form expression for the bandwidth value, and some suggest a bandwidth value based on an iterative scheme or a bandwidth value obtained from solving an ancillary optimization problem.
2. Selection methods that are based on edge-detection: These methods use edge-detection techniques to determine the boundary of the data. The boundary points are used to generate pseudo-outliers that lie just

beyond the boundary of the data. The pseudo-outliers along with the training data enables cross-validation to be used to determine a suitable bandwidth. In some methods, pseudo-inliers that mimic the training data are also generated and cross-validation based on the quality of fit on both the pseudo-outliers and the pseudo-inliers is used to determine a bandwidth.

### 3.1. Intrinsic Methods

Common intrinsic methods for bandwidth selection for SVDD include: the coefficient of variation method (CV) [5], the distance to farthest neighbor method (DFN) [20], the peak criterion method [7, 10] and the modified mean criterion method ( $\text{mean}_2$ ) [8] (see also [3]). For the rest of this section, we assume that we are given data  $x_1, \dots, x_N \in \mathbb{R}^p$  and that  $K(s) = (k_{ij}(s))_{i,j=1}^N = \left( \exp\left(-\frac{\|x_i - x_j\|^2}{2s^2}\right) \right)_{i,j=1}^N$  is the corresponding kernel matrix.

#### 3.1.1. Coefficient of Variation method [5]

The coefficient of variation (CV) method selects the bandwidth that maximizes the following objective function:

$$f(s) = \frac{V(s)}{\kappa(s) + \epsilon}. \quad (17)$$

Here,  $V(s)$  is the variance of the non diagonal elements of the kernel matrix and  $\kappa(s)$  is their mean.  $\epsilon$  is a pre-selected small quantity, which is added to the denominator for numerical stability. The optimization can be performed using gradient based methods. Because the computation of the objective function entails an  $\mathcal{O}(N^2)$  computational cost, this method is computationally expensive for large data.

#### 3.1.2. Distance to Farthest Neighbor Method [20]

The distance to farthest neighbor method (DFN) chooses the bandwidth that maximizes the following objective function:

$$f(s) = \frac{1}{N} \sum_{i=1}^N \max_{j \neq i} k_{ij}(s) - \frac{1}{N} \sum_{i=1}^N \min_j k_{ij}(s). \quad (18)$$

The computation of the objective function entails an  $\mathcal{O}(N^2)$  computational cost, so this method is also computationally expensive for large data.

### 3.1.3. Peak Criterion Method[7]

For a given bandwidth, say  $s$ , let  $\theta(s)$  be the optimal value of the objective function that defines the SVDD problem. The peak criterion method chooses the bandwidth as the smallest zero of the second derivative of  $\theta(s)$ . The second derivative is computed numerically by finite differences, by varying  $s$  over a grid of values and solving the optimization problem that defines SVDD for each value in the grid. The choice of the grid is very important because most solvers run very slowly when supplied with a bandwidth value much smaller than the scale of the values in the data. You also need to make sure the grid is fine enough so that the second derivative can be computed to a reasonable level of approximation. However making the grid fine means you have to solve the SVDD optimization a large number of times which is computationally expensive.

### 3.1.4. Modified mean Criterion [8]

The modified mean ( $\text{mean}_2$ ) criterion method suggests a bandwidth which has a closed form in terms of the data. The suggested bandwidth is given by

$$s = \sqrt{\frac{2N \sum_{i=1}^p \sigma_i^2}{(N-1)}} \sqrt{\frac{1}{\ln(\frac{N-1}{\delta^2})}}.$$

Here,  $\sigma_i^2$  is the variance of the  $i^{\text{th}}$  variable and

$$\delta = -0.14818008\phi^4 + 0.284623624\phi^3 - 0.252853808\phi^2 + 0.159059498\phi - 0.001381145$$

where  $\phi = \frac{1}{\ln(N-1)}$ .

The cost of the preceding computation is only  $\mathcal{O}(Np)$ .

## 3.2. Methods that are based on Edge Detection

### 3.2.1. Self-Adaptive Edge Detection Method [17]

The current state of the art for a bandwidth selection method based on edge detection is the self-adaptive data shifting method (SADS). This is a method that uses K-nearest-neighbors (KNN) (with  $5 \log_{10}(N)$  neighbors) to detect the points that lie at the boundary (edge) of the data along with the outward normals at these points. This method uses the boundary points to create pseudo-outliers that lie just beyond the data boundary. The next step in this method is to estimate the direction of the maximum density for each point in the data and use these directions to create a dataset of pseudo-inliers

that closely mimics the training data. Having generated the pseudo-outliers and pseudo-inliers, the method uses cross-validation to select the bandwidth that provides the best fit both on the pseudo-outliers and the pseudo-inliers. The cross-validation is done by considering candidate bandwidth values over a set that varies uniformly in the logarithmic scale. The authors of [17] choose values of  $\sigma = \sqrt{2}s$  that lie in the set  $\{10^{-4}, 10^{-3}, 10^{-2}, \dots, 10^4\}$ . SADS is a “fully automatic” method, the choice of the number of neighbors and the search grid is a part of the definition of SADS.

We have observed that in practice the default value of the number of neighbors suggested by the authors of [17] is inappropriate for many datasets. Also the default grid suggested in [17] is inadequate for many datasets. The logarithmic scale makes it likely that we skip the region near good bandwidth values for many datasets, for example the method evaluates  $\sigma$  values  $10^3 = 1000$  and  $10^4 = 10000$  in succession. There will be many datasets for which a good value will lie between these two values and neither of the suggested values are appropriate. We will give an example of one such dataset later.

#### 4. Evaluating the Trace Criterion Method

In this section we compare the trace criterion method with the five bandwidth selection techniques mentioned in the previous section. The competing bandwidth selection methods are tested on different types of datasets, both simulated and real, to cover the kind of data that can arise in various situations. A 32.0 GB machine with 4 cores at 3.40 GHz was used for all analysis below.

##### 4.1. Choice of Data

In the SVDD formulation, the objective function depends on the data through the distance matrix. So it is natural to consider cases that lead to different types of distance matrices. For example the distribution of pairwise distances of a data where the observations lie in different clusters tends to be multimodal in contrast to data where the observations are concentrated in one connected set [3].

Another important factor than can impact the performance of different methods is the dimension of the data. Methods that work well for two-dimensional data might not work well for high-dimensional data, so it is important to compare the methods on data of different dimensions. For two-dimensional data we can easily gauge whether a bandwidth leads to a

reasonable description by visual inspection. However this cannot be done for higher dimensions. For high-dimensional data we have two choices: 1) we can use labeled data where we have reasons to believe that observations in the data corresponding to distinct labels lie in geometrically separate regions of space, or, 2) we can use simulated data where the ground truth is known.

With the preceding factors in mind we evaluate the trace criterion on the following four types of data:

- Connected two-dimensional data: These are data that have two variables, and the observations lie in a connected set, that is, there are no natural clusters in the data.
- Disconnected two-dimensional data: These are data that have two variables and the observations can be naturally divided into multiple clusters.
- Higher-dimensional labeled real data: These are high-dimensional real data with multiple labels. We choose a subset of the data that corresponds to one label (usually the dominant label) and we see how well the SVDD fit that corresponds to a particular bandwidth separates our selected label from the other labels.
- High-dimensional simulated data: We simulate high-dimensional data from various high-dimensional geometric shapes. We consider the case where the observations are *connected* and the case where the observations lie in multiple clusters. We simulate the data for different dimensions and study the impact of dimension on the different bandwidth selection methods.

#### 4.2. Comparison on two-dimensional data

In this section we compare the performance of the different bandwidth selection methods on various two-dimensional data. The two dimensional case is special because we can easily make a judgement on the quality of description provided by a bandwidth by visual inspection. We will compare the different methods on a variety of *connected* data, i.e., data without any obvious clusters, and data with multiple clusters.

#### 4.2.1. Data Description

This section compares the trace criterion with other bandwidth criteria using two-dimensional connected data. Such data have no clusters. We use the star-shaped data and banana-shaped data, and we train an SVDD model by using the bandwidth value obtained by the peak, modified mean, trace criteria, CV, DFN and SADS. To evaluate the results, we scored the bounding rectangle of the data by dividing it into a  $200 \times 200$  grid and plotted the inlier region. With a good bandwidth value, the inlier region that is obtained from scoring should match the geometry of the training data.

#### 4.2.2. Scoring Results

Figures 2 and 3 display the results, along with the bandwidth value. The inlier region is shaded darkly. For banana-shaped data, the scoring results indicate that the bandwidth value obtained using all methods except DFN provide good-quality data description. The values of bandwidth  $s$  obtained using CV, peak and trace are close. For star-shaped data, CV and trace provide the best data description.

**Figure 2:** Results for two-dimensional connected data (Banana-shaped data)

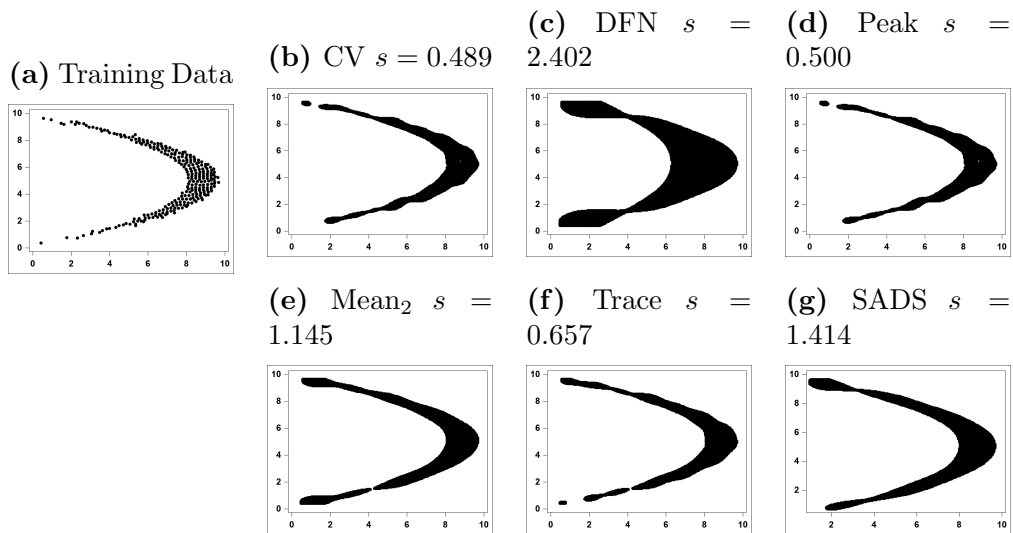
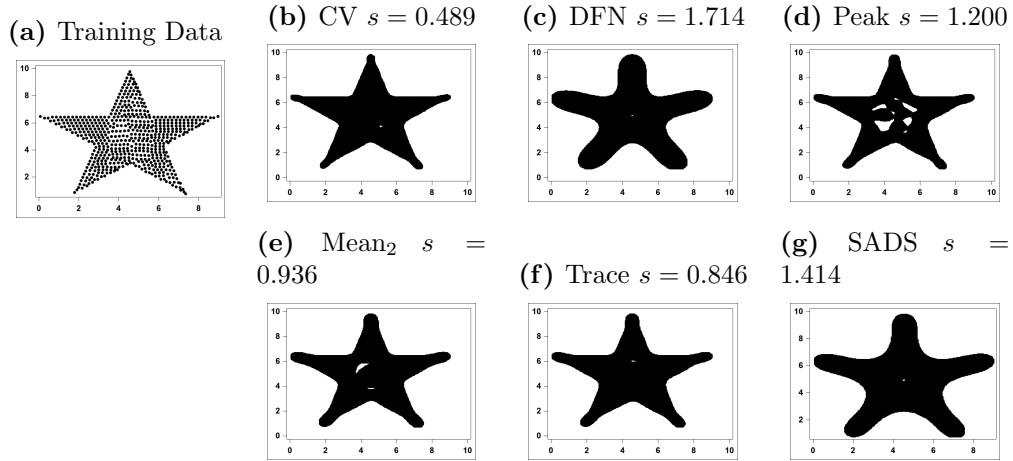




**Figure 3:** Results for Two-Dimensional Connected Data (Star-shaped Data)



### 4.3. Comparison Using Two-Dimensional Disconnected Data

#### 4.3.1. Data Description

This section compares bandwidth selection methods using two-dimensional data that lie across multiple clusters. We have observed that computing a good bandwidth value for such data is more difficult than for connected data. Since the data are two-dimensional, we can visually judge the quality of results. To evaluate the results, we scored the bounding rectangle of the data by dividing it into a  $200 \times 200$  grid. With a good bandwidth value, the inlier region obtained from scoring should match the geometry of the training data. We use the following three data sets for evaluations:

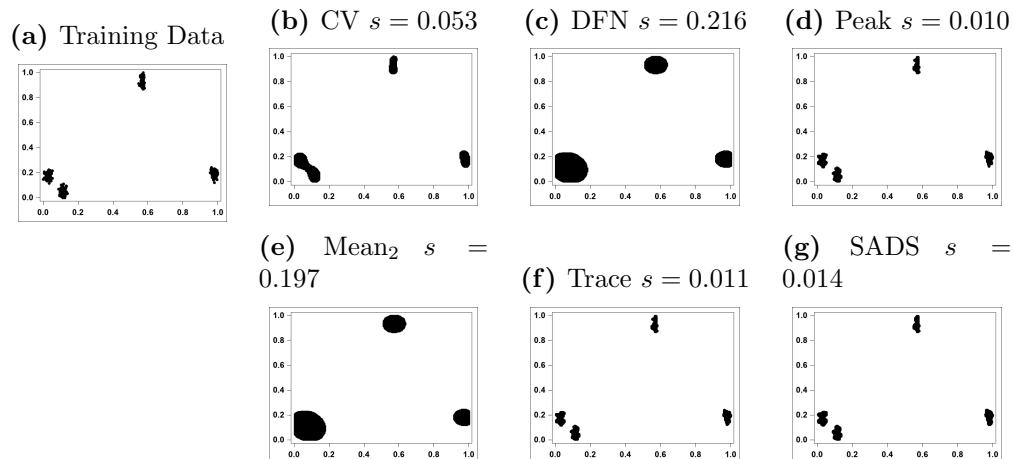
- The refrigerant data which consists of four clusters [6]
- A simulated “two-donut and a circle” data set, which consists of two donut-shaped clusters and one circular cluster

Figures 4 and 5 display the results, along with the bandwidth value.

#### 4.3.2. Scoring Results

For the refrigerant data, the data description that is obtained using peak, trace and SADS is able to separate out all four clusters, whereas the description obtained using the modified mean criterion, CV and DFN merges the two clusters that lie close to each other.

**Figure 4:** Results for two-dimensional disconnected data (Refrigerant Data)

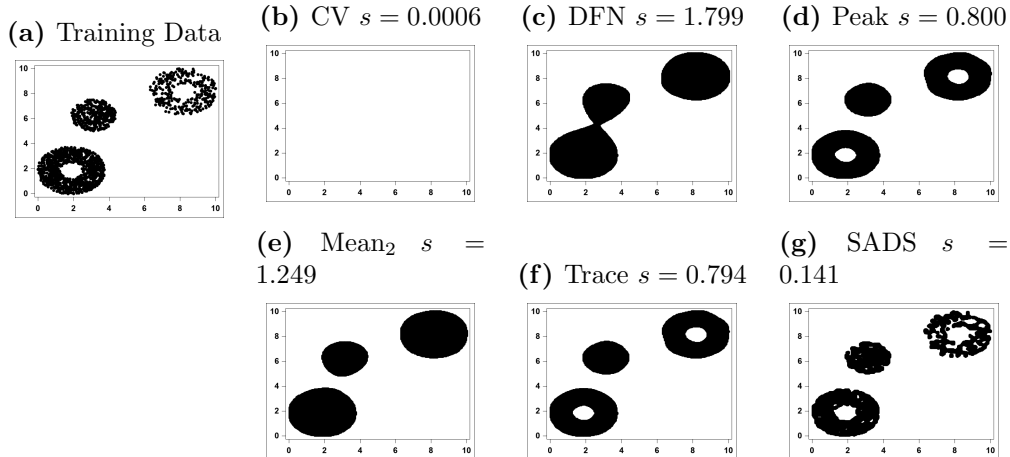


For the “two-donut and a circle” data set, the peak and trace methods choose an appropriate bandwidth and deliver the best visual results. The DFN and modified mean methods both choose a large bandwidth, while CV and SADS select a small bandwidth.

#### 4.4. Comparison Using High-Dimensional Data

Comparing the different criteria for high-dimensional data is much more difficult than comparing them for two-dimensional data. In two-dimensional data, the quality of the result can be easily judged by looking at the plot of the scoring results. But this is not possible for high-dimensional data. For the purpose of evaluation, we selected labeled high-dimensional data that have a dominant class. We used SVDD on a subset of the dominant class to obtain a description of it, and then we scored the rest of the data to evaluate the criteria. We expected the points in the scoring data set that correspond to the dominant class to be classified as inliers and all other points to be classified as outliers. Because the data are labeled, we could also use cross validation to determine the bandwidth that best describes the dominant class in the sense of maximizing a measure of fit, such as the  $F_1$  score. So in this section we compare the bandwidths that are suggested by the different unsupervised criteria with the bandwidth that is obtained through cross validation for various benchmark data sets. The results are summarized in Table 1. The benchmark data sets used for the analysis are described in sections 4.4.1.

**Figure 5:** Results for two-dimensional disconnected data (Two Donuts and a circle data). Note that the CV bandwidth is very small, almost zero, thus, none of the observations in the scoring grid are labeled as inliers.



#### 4.4.1. Data Description

*Shuttle Data.* This data set consists of measurements made on a shuttle. The data set contains nine numeric attributes and one classification attribute. Of 58,000 total observations, 80% belong to class 1. A random sample of 2,000 observations belonging to class 1 was selected for training, and the remaining 56,000 observations were used for scoring. This data set is from the UC Irvine Machine Learning Repository [4].

*Tennessee Eastman Data.* This data set was generated using MATLAB simulation code, which provides a model of an industrial chemical process. The data were generated for normal operations of the process and 20 faulty processes. Each observation consists of 41 variables, out of which 22 were measured continuously every 6 seconds on average and the remaining 19 were sampled at a specified interval of every 0.1 or 0.25 hours. From the simulated data, we created an analysis data set that uses the normal operations data of the first 90 minutes and data that correspond to faults 1 through 20. A data set that contains observations of normal operations was used for training. Scoring was performed to determine whether the model could

**Table 1:** Results for high-dimensional Data

Method	Shuttle		Tennessee Eastman	
	$F_1$	$s$	$F_1$	$s$
Cross-Validation	0.96	17.0	0.18	12.25
CV	0.93	9.2	0.15	7.3
DFN	0.91	225.0	0.17	24.1
Peak	0.81	5.0	0.15	7.0
Modified Mean	0.96	17.2	0.18	11.4
SADS	0.95	14.1	0.18	14.1
Trace	0.96	13.1	0.18	11.2

accurately classify an observation as belonging to normal operation of the process. The MATLAB simulation code is available at [11].

#### 4.4.2. Scoring Results

The results outlined in table 1 show that the bandwidths by the proposed trace, modified mean and SADS methods each have a  $F_1$  measure value that is almost identical to that given by the bandwidth selected using cross validation.

#### 4.5. Comparison Using Simulated Data

In this section, we present results of a simulation study that we conducted to compare performance of different methods. The simulations were performed to generate training data with a known geometry. The inlier region corresponding to a good bandwidth selection method should exactly match the known true geometry of underlying data. And we can use the discrepancy from the true geometry to rank different bandwidth selection methods.

The data dimensions were varied between 2 and 40. We conducted five simulation studies. Table 2 provides details of these studies.

##### 4.5.1. Evaluation Using Two-Dimensional Polygons

In this section, we measure the performance of the trace criterion when it is applied to randomly generated polygons. Given the number of ver-

**Table 2:** Simulation study description

Simulation	Data Dimension	Number of data sets	Description
Two-dimensional polygons	2	500	Polygons with varying number of vertices and length of sides
Hypercubes	5 to 40 in increments of 5	200	Single hypercube used for training
Hyperspheres	5 to 40 in increments of 5	200	Single hypersphere used for training
High-dimensional disconnected data with multiple hyperspheres	5 to 40 in increments of 5	160	Each training data set contains multiple disjoint hyperspheres, either 5 or 10.
High-dimensional disconnected data with multiple hypercubes	5 to 40 in increments of 5	160	Each training data set contains multiple disjoint hypercubes, either 5 or 10.

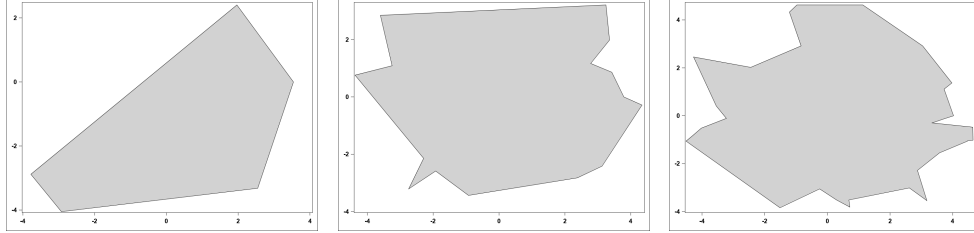
tices,  $k$ , we generate the vertices of a polygon in the anticlockwise sense as  $r_1 \exp i\theta_{(1)}, \dots, r_k \exp i\theta_{(k)}$ . Here  $\theta_{(1)} = 0$  and  $\theta_{(i)}$  for  $i = 2, \dots, n$  are the order statistics of an i.i.d sample that is uniformly drawn from  $(0, 2\pi)$ . The  $r_i$  are uniformly drawn from an interval  $[r_{\min}, r_{\max}]$ .

For this simulation, we chose  $r_{\min} = 3$  and  $r_{\max} = 5$  and varied the number of vertices from 5 to 30. We generated 20 random polygons for each vertex size. Having determined a polygon, we randomly sampled 1200 points uniformly from the interior of the polygon and used trace criterion and this sample to determine a bandwidth value. Figure 6 shows three random polygons.

The box and whiskers plot in Figure 7a summarizes the simulation study results. The X-axis shows the number of vertices of the polygon and Y-axis shows the  $F_1$  score. The bottom and the top of the box shows the first and the third quartile values. The ends of the whiskers represent the minimum and the maximum values of the  $F_1$  score. The plot shows that the  $F_1$  score is greater than 0.9 across all values of number of vertices for all methods except CV. Because the complexity of the polygon increases as the number of vertices increases, we observed that the  $F_1$  score decreased slightly. The

**Figure 6:** Random polygons

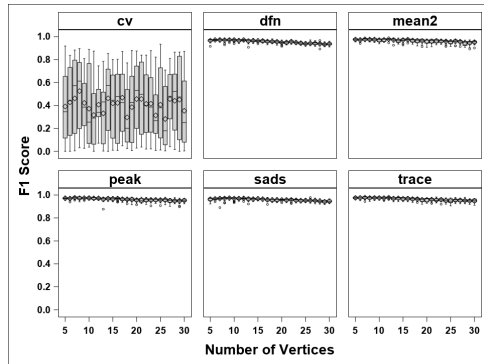
(a) Number of Vertices = 5 (b) Number of Vertices = 15 (c) Number of Vertices = 30



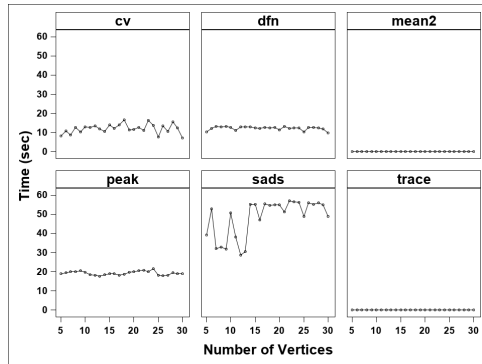
fact that  $F_1$  score is always greater than 0.9 provides necessary evidence that the trace criterion performs well. Figure 7b summarizes the time performance of each method. For all number of vertices, modified mean and trace outperform CV, DFN, peak and SADS, showing that trace is competitive in both accuracy and performance.

**Figure 7:** Simulation results for random polygons

(a) Accuracy using random polygons



(b) Timing using random polygons



#### 4.5.2. Evaluation Using Hyperspheres

In this section, we evaluate the trace criterion by using spherical data of varying dimensions. The observations in such spherical data (or hypersphere) are uniformly distributed. We use scoring to evaluate the quality of the data description that is obtained using the trace criterion bandwidth value. The

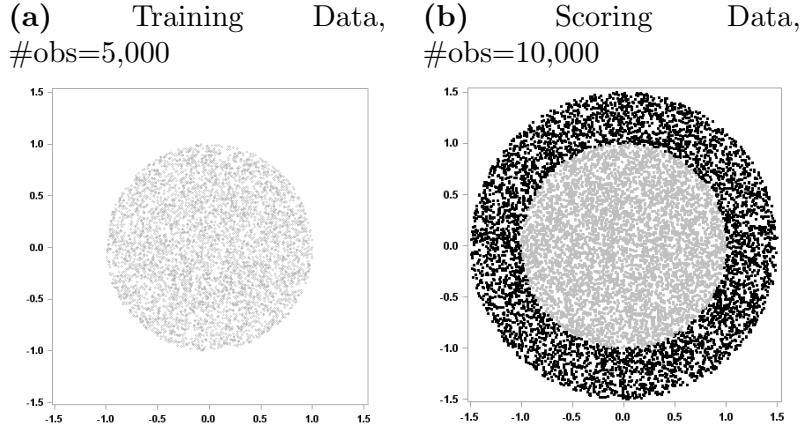
scoring data set consists of 50% *inlier* observations, which are uniformly distributed inside the training sphere and 50% *outlier* observations, which are uniformly distributed outside the sphere. The points outside the sphere lie in a narrow annular ring, just outside the sphere. Figure 8 illustrates two variables in the training and scoring data. The rationale behind creating such scoring data set is that if the bandwidth value is good, then the data description that is obtained using such a value should be able to discriminate between observations that are inside and observations that are just outside the sphere. We varied the hypersphere dimension from 5 to 40 in increments of 5. For each dimension, 25 sets of training and scoring data sets were simulated. We computed the  $F_1$  measure for each data set to determine the quality of data description. The width of the annular region was half the radius of the sphere.

Figure 9a shows a box-and-whiskers plot of the  $F_1$  measure for various values of data dimension. The  $F_1$  measure decreases as the number of variables (the data dimension) increases from 5 to 40. For CV, DFN, peak and trace methods, the  $F_1$  measure is consistently above 0.9 for all simulated data sets across different dimensions. While for the modified mean method, the  $F_1$  measure dropped rapidly with the increase in the hypersphere dimension. The SADS method fails to produce a bandwidth value for dimensions greater than 25. The best observed bandwidth for these high dimensional spheres is  $0.6 < s < 1$ . Note that this range of values is not in the SADS grid  $[10^{-4}\sqrt{2}, 10^{-3}\sqrt{2}, \dots, 10^4\sqrt{2}]$ . This is the greatest disadvantage of SADS; if the best bandwidth value does not lie near the specified grid points, only pseudo-outliers will be generated resulting in a failure to produce a bandwidth. Figure 9b shows the amount of time taken to compute each bandwidth value. Note that the trace and modified mean bandwidths are computed in under 1 second, while CV, DFN, peak, and SADS are computed in over 20 seconds. These observations confirm that a bandwidth value that is obtained using the trace criterion provides competitive-quality data description with competitive-time performance.

#### 4.5.3. Evaluation Using Hypercubes

In this section, we evaluate the trace criterion using cube-shaped data of varying dimensions. The observations in such cubic data (or hypercube) are uniformly distributed. We used scoring to evaluate the quality of data description that was obtained using the trace criterion bandwidth value. The scoring data set consists of 50% *inlier* observations, which are uniformly

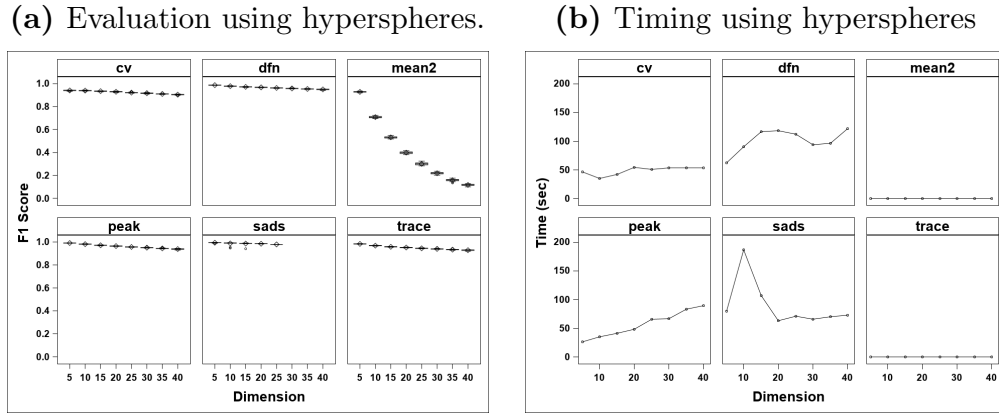
**Figure 8:** Evaluation using hyperspheres



distributed inside the training cube and 50% *outlier* observations which are uniformly distributed outside the cube. The points outside the cube lie in a narrow frame, just outside the cube. Figure 10 illustrates the two variables in the training and scoring data. The rationale behind creating such a scoring data set is that if the bandwidth value is good, then the data description that is obtained using such a value should be able to discriminate between observations that are inside and observations that are just outside the cube. We varied the hypercube dimension from 5 to 40 in increments of 5. For each dimension, 25 sets of training and scoring data sets were simulated. The width of the frame was 0.25 times the length of the cube. We computed the  $F_1$  measure for each data set to determine the quality of data description. Figure 11a shows a box-and-whiskers plot of the  $F_1$  measure for various values of data dimension. We observed a similar pattern as in the hypersphere case. The  $F_1$  measure decreases as the number of variables (the data dimension) increases from 5 to 40. For CV, DFN, peak and trace method, the  $F_1$  measure is consistently above 0.7 for all simulated data sets across different dimensions. While for modified mean method, the  $F_1$  measure value dropped rapidly with the increase in the hypercube dimension. The SADS method fails to converge to a bandwidth for all dimensions greater than 25. This observation confirms that bandwidth values obtained using the trace criterion provide a much better-quality data description than the modified mean and SADS criteria provide. Moreover, figure 11b shows that the modified mean and trace methods compute the bandwidth in less time than CV, DFN, peak,

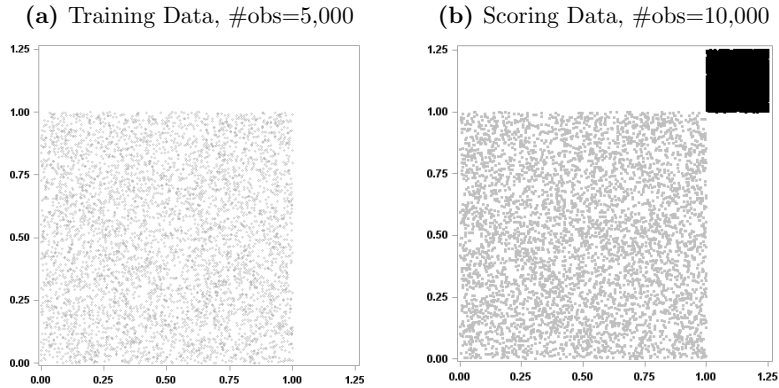


**Figure 9:** Simulation results for hyperspheres. SADS fails to obtain a bandwidth value for all dimensions greater than 25



and SADS, thus illustrating that the trace criteria is competitive in both accuracy and performance.

**Figure 10:** Evaluation using hypercubes

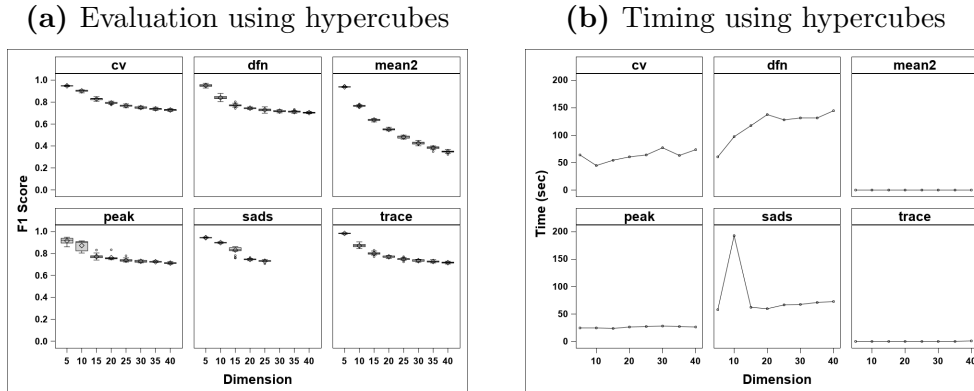


#### 4.5.4. Evaluation using Multiple Hyperspheres

In this section, we use high-dimensional disconnected data to evaluate the performance of the trace criteria. The training data consist of two or more disjoint hyperspheres used earlier in section 4.5.2.

We evaluated the bandwidth criteria by using data sets that contain multiple numbers of spheres. The number of spheres in a data set was either 5

**Figure 11:** Simulation results using hypercubes. Peak fails to obtain a bandwidth value for 50% of cubes of dimensions 20 or greater. SADS fails for 100% of cubes of dimensions 30 or greater.



or 10, and the data dimension ranged from 5 to 40. For each combination of data dimension and number of spheres, we used different seed values to generate 10 different sets of training and scoring data sets. Figure 12 illustrates sample training and scoring data sets that have five spheres and use two dimensional data.

For each simulation run, we computed the  $F_1$  measure. Figure 13 and Figure 14 provide the box-and-whiskers plot of the  $F_1$  measure for simulations results that were obtained using 5 and 10 hyperspheres respectively. The CV, peak, and trace criteria perform well on this simulation setting, giving F1 scores consistently higher than 0.8. Additionally, CV frequently fails to converge to a bandwidth value, and SADS does not provide any bandwidth values for spheres with dimension greater than 20. Trace outperforms both CV and peak in time performance.

#### 4.5.5. Evaluation Using Multiple Hypercubes

We evaluated the bandwidth criteria by using data sets that contain multiple numbers of cubes. The number of cubes in a data set was either 5 or 10, and the data dimension was varied between 5 and 40 in increments of 5. For each combination of data dimension and number of cubes, we generated 10 different sets of training and scoring data sets by different seed value. Figure 3 illustrates sample training and scoring data set that have five cubes and use two-dimensional data.

**Figure 12:** Evaluation using multiple hyperspheres

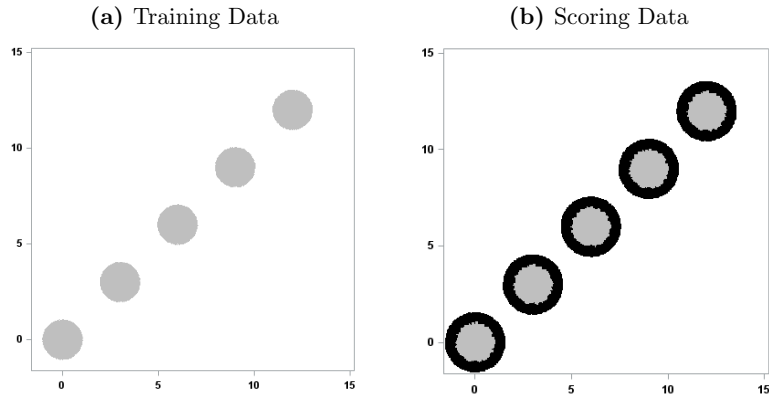
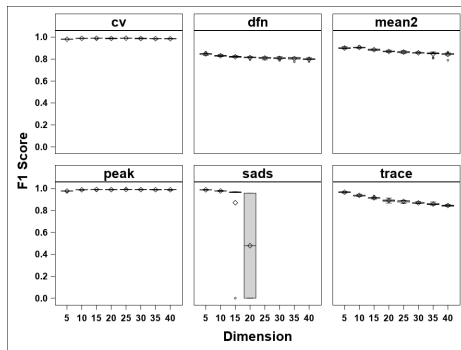


**Figure 13:** Simulation results using 5 hyperspheres. CV fails to converge to a bandwidth value for 60% of hyperspheres of dimensions 5 or greater. SADS fails to converge for 80% of hyperspheres of dimension 20 and for 100% of hyperspheres of dimensions 25 or greater.

**(a) Evaluation using 5 hyperspheres.**



**(b) Timing using 5 hyperspheres**

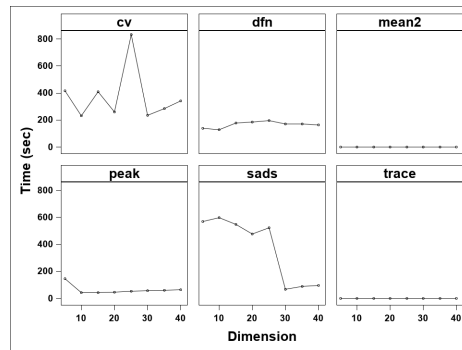
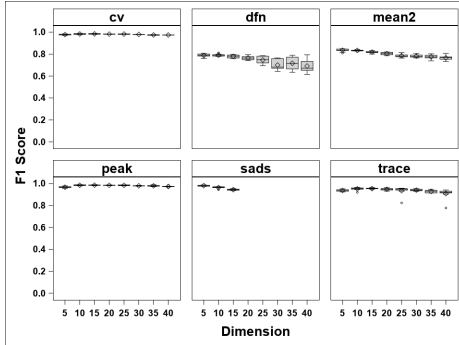


**Figure 14:** Simulation results using 10 hyperspheres. CV fails to converge to a bandwidth value for 70% of hyperspheres of dimensions 5 or greater. SADS fails to converge for 100% of hyperspheres of dimensions 20 or greater.

(a) Evaluation using 10 hyperspheres.



(b) Timing using 10 hyperspheres

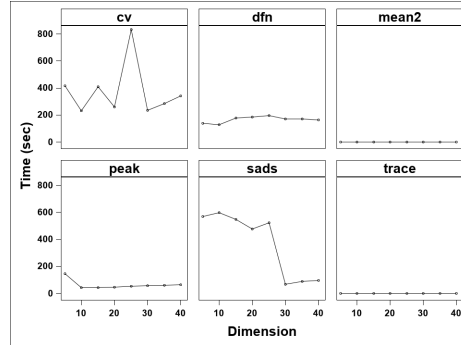
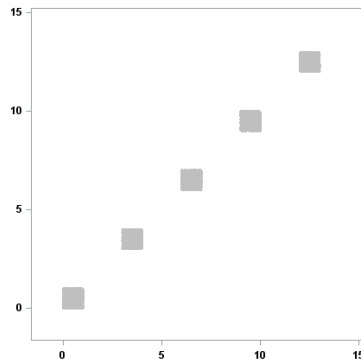


**Table 3:** Evaluation using multiple hypercubes

(a) Training Data



(b) Scoring Data

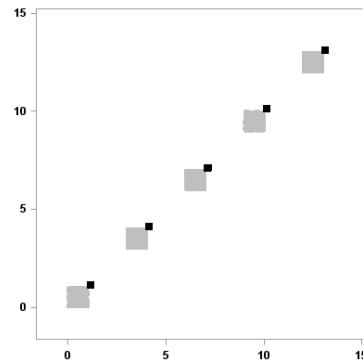
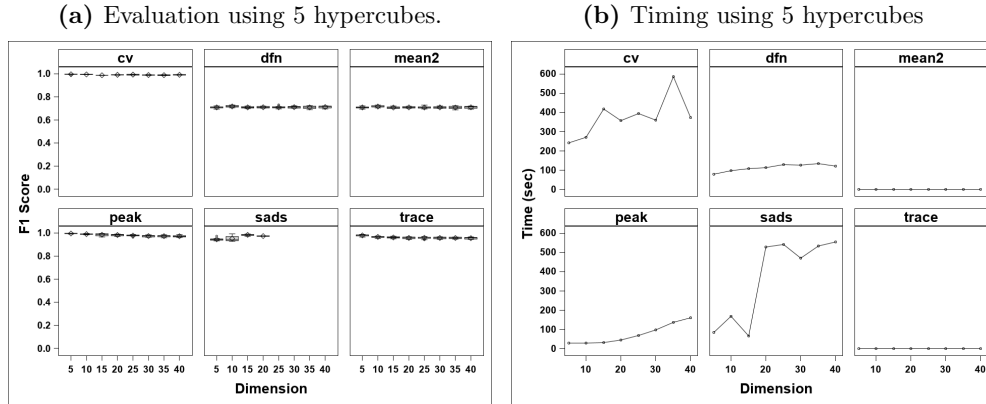
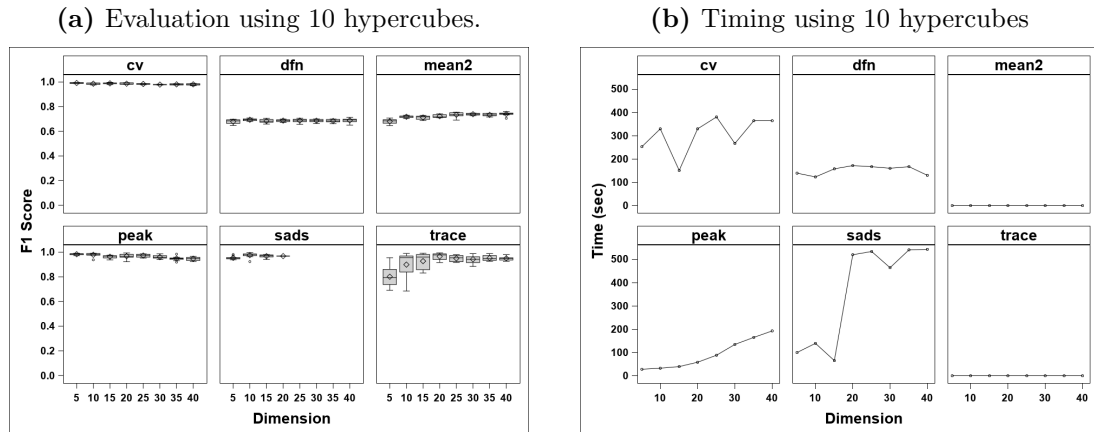


Figure 15 and Figure 16 provide the box-and-whiskers plot of the  $F_1$  measure for simulations results that were obtained using 5 and 10 hypercubes respectively. The CV, peak and trace criterion have the best accuracy performance in this simulation setting. However, CV frequently fails to converge to a bandwidth. SADS does not provide a bandwidth for dimensions greater than 20. Additionally, of the three methods with best accuracy performance, the trace criteria has the best timing performance.

**Figure 15:** Simulation results using 5 hypercubes. CV fails to converge to a bandwidth value for 60% of hypercubes of dimension 5 or greater. SADS fails to converge for 100% of hypercubes of dimension 25 or greater.



**Figure 16:** Simulation results using 10 hypercubes. CV fails to converge to a bandwidth value for 60% of hypercubes of dimension 5 or greater. SADS fails to converge for 100% of hypercubes of dimension 25 or greater.

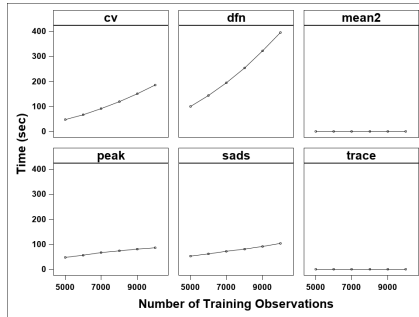


#### 4.5.6. Evaluation using Increasing Number of Training Observations

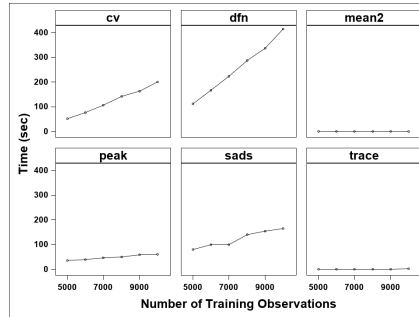
We evaluated the performance of the hypersphere, hypercube, multi-hypersphere and multi-hypercube simulations as the number of training observations  $N$  increases. We varied  $N$  between 5000 and 10000 in increments of 5000. For each simulation and for each value of  $N$ , we generated 5 different sets of training and scoring data sets using different seed values.

**Figure 17:** Timing results for high-dimensional simulated data

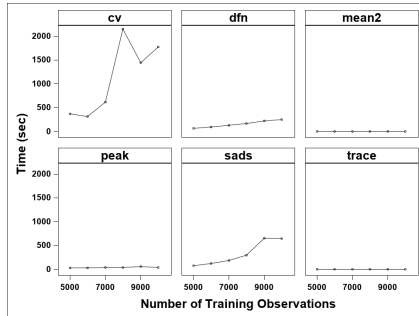
(a) Timing using hyperspheres with dim 20



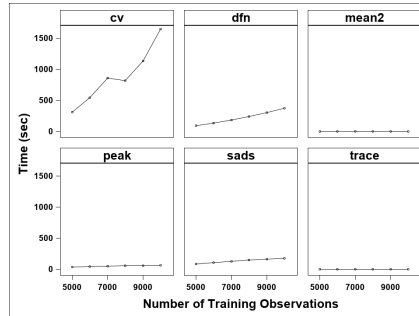
(b) Timing using hypercubes with dim 20



(c) Timing using 5 hyperspheres with dim 20



(d) Timing using 5 hypercubes with dim 20



The  $F_1$  scores corresponding with each bandwidth criteria remained largely unchanged as  $N$  increased with the exception of CV and SADS, which failed to converge to a bandwidth value for approximately 50% of the data sets with  $N > 5000$ . Figure 17 shows that for all four simulations, the modified mean and trace criteria outperform CV, DFN, peak and SADS as the number of training observations increases both in terms of quality of results and the time taken for computation.

## **5. Conclusion**

The trace criterion for computing the bandwidth value of a Gaussian kernel for SVDD, as proposed in this paper, exploits the low-rank representation of the kernel matrix to suggest a bandwidth value. Several evaluations that use synthetic and real-life data sets indicate that the bandwidth value that is obtained using the trace criterion provides similar or better results compared to existing methods and it can be computed quickly even for large datasets. In particular the trace criterion method provides the best results when data are high-dimensional and disjoint.

## **Acknowledgement**

Authors would like to thank Anne Baxter, Principal Technical Editor at SAS, for her assistance in creating this manuscript.

## References

- [1] AGGARWAL, C. C. *Data mining: the textbook*. Springer, 2015.
- [2] CAMCI, F., AND CHINNAM, R. B. General support vector representation machine for one-class classification of non-stationary classes. *Pattern Recognition* 41, 10 (2008), 3021–3034.
- [3] CHAUDHURI, A., KAKDE, D., SADEK, C., GONZALEZ, L., AND KONG, S. The mean and median criteria for kernel bandwidth selection for support vector data description. In *2017 IEEE International Conference on Data Mining Workshops (ICDMW)* (Nov 2017), pp. 842–849.
- [4] DUA, D., AND GRAFF, C. UCI machine learning repository, 2017.
- [5] EVANGELISTA, P. F., EMBRECHTS, M. J., AND SZYMANSKI, B. K. Some properties of the Gaussian kernel for one class learning. In *Artificial Neural Networks–ICANN 2007*. Springer, 2007, pp. 269–278.
- [6] HECKERT, N. A., AND FILLIBEN, J. J. NIST handbook 148: DATAPLOT reference manual, Volume I: Commands. <http://www.itl.nist.gov/div898/software/dataplot/>, 2000. [Online; accessed 4-August-2017].
- [7] KAKDE, D., CHAUDHURI, A., KONG, S., JAHJA, M., JIANG, H., AND SILVA, J. Peak Criterion for Choosing Gaussian Kernel Bandwidth in Support Vector Data Description. In *2017 IEEE International Conference on Prognostics and Health Management (ICPHM) (PHM2017)* (2017). [Online preprint.] Available: <https://arxiv.org/abs/1602.05257>.
- [8] LIAO, Y., KAKDE, D., CHAUDHURI, A., JIANG, H., SADEK, C., AND KONG, S. A new bandwidth selection criterion for using SVDD to analyze hyperspectral data. In *Algorithms and Technologies for Multispectral, Hyperspectral, and Ultraspectral Imagery XXIV* (2018), vol. 10644, International Society for Optics and Photonics, p. 106441M. [Online preprint.] Available: <https://arxiv.org/abs/1803.03328>.
- [9] MAGNUS, J. R., AND NEUDECKER, H. Matrix differential calculus with applications in statistics and econometrics. *Wiley series in probability and mathematical statistics* (1988).



- [10] PEREDRIY, S., KAKDE, D., AND CHAUDHURI, A. Kernel bandwidth selection for SVDD: The sampling peak criterion method for large data. In *2017 IEEE International Conference on Big Data (Big Data)* (Dec 2017), pp. 3540–3549.
- [11] RICKER, N. L. Tennessee Eastman challenge archive, matlab 7.x code. <http://depts.washington.edu/control/LARRY/TE/download.html>, 2002. [Online; accessed 21-March-2016].
- [12] SANCHEZ-HERNANDEZ, C., BOYD, D. S., AND FOODY, G. M. One-class classification for mapping a specific land-cover class: SVDD classification of fenland. *Geoscience and Remote Sensing, IEEE Transactions on* 45, 4 (2007), 1061–1073.
- [13] SAS INSTITUTE INC. SAS® Visual Data Mining and MachineLearning 8.4: Procedures. [https://go.documentation.sas.com/?docsetId=casml&docsetTarget=casml\\_svdd\\_details09.htm&docsetVersion=8.4&locale=en#casml.svdd.bw\\_trace](https://go.documentation.sas.com/?docsetId=casml&docsetTarget=casml_svdd_details09.htm&docsetVersion=8.4&locale=en#casml.svdd.bw_trace).
- [14] SCHÖLKOPF, B., WILLIAMSON, R. C., SMOLA, A. J., SHAWE-TAYLOR, J., AND PLATT, J. C. Support vector method for novelty detection. In *Advances in neural information processing systems* (2000), pp. 582–588.
- [15] SUKCHOTRAT, T., KIM, S. B., AND TSUNG, F. One-class classification-based control charts for multivariate process monitoring. *IIE transactions* 42, 2 (2009), 107–120.
- [16] TAX, D. M., AND DUIN, R. P. Support vector data description. *Machine learning* 54, 1 (2004), 45–66.
- [17] WANG, S., LIU, Q., ZHU, E., PORIKLI, F., AND YIN, J. Hyperparameter selection of one-class support vector machine by self-adaptive data shifting. *Pattern Recognition* 74 (2018), 198–211.
- [18] WIDODO, A., AND YANG, B.-S. Support vector machine in machine condition monitoring and fault diagnosis. *Mechanical Systems and Signal Processing* 21, 6 (2007), 2560–2574.
- [19] WILLIAMS, C. K. I., AND SEEGER, M. Using the Nyström method to speed up kernel machines. In *Advances in Neural Information Processing*

*Systems 13*, T. K. Leen, T. G. Dietterich, and V. Tresp, Eds. MIT Press, 2001, pp. 682–688.

- [20] XIAO, Y., WANG, H., ZHANG, L., AND XU, W. Two methods of selecting Gaussian kernel parameters for one-class svm and their application to fault detection. *Knowledge-Based Systems 59* (2014), 75–84.
- [21] YPMA, A., TAX, D. M., AND DUIN, R. P. Robust machine fault detection with independent component analysis and support vector data description. In *Neural Networks for Signal Processing IX, 1999. Proceedings of the 1999 IEEE Signal Processing Society Workshop*. (1999), IEEE, pp. 67–76.
- [22] ZHANG, K., TSANG, I. W., AND KWOK, J. T. Improved Nyström low-rank approximation and error analysis. In *Proceedings of the 25th international conference on Machine learning* (2008), ACM, pp. 1232–1239.